Information–disturbance tradeoff in continuous-variable Gaussian systems

Marco G. Genoni and Matteo G. A. Paris*

Dipartimento di Fisica dell'Università di Milano, Milano, Italia

(Received 15 January 2006; published 6 July 2006)

We address the information–disturbance tradeoff for state measurements on continuous variable Gaussian systems and suggest minimal schemes for implementations. In our schemes, the symbols from a given alphabet are encoded in a set of Gaussian signals which are coupled to a probe excited in a known state. After the interaction the probe is measured, in order to infer the transmitted state, while the conditional state of the signal is left for the subsequent user. The schemes are minimal, i.e., involve a single additional probe, and allow for the nondemolitive transmission of a continuous real alphabet over a quantum channel. The tradeoff between information gain and state disturbance is quantified by fidelities and, after optimization with respect to the measurement, analyzed in terms of the energy carried by the signal and the probe. We found that transmission fidelity only depends on the energy of the signal and the probe, whereas estimation fidelity also depends on the alphabet size and the measurement gain. Increasing the probe energy does not necessarily lead to a better tradeoff, the most relevant parameter being the ratio between the alphabet size and the signal width, which in turn determine the allocation of the signal energy.

PACS number(s): 03.67.Hk, 03.65.Ta

I. INTRODUCTION

In a multiuser transmission line each user should decode the transmitted symbol and leave the carrier for the subsequent user. Therefore, some device is needed that, at each use of the channel, permits the retrieval of information without the destruction of the carrier. In a quantum channel symbols are encoded in states of a physical system and therefore the ultimate bounds on the channel performances are posed by quantum mechanics. Indeed, any measurement aimed to extract information on a quantum state alters the state itself, i.e., produces a disturbance [1]. Quantum information, in fact, cannot be perfectly copied, neither locally [2] nor at distance [3]. Overall, there is an information–disturbance tradeoff which unavoidably limits the accuracy independently on the coding scheme [4].

Several approaches have been proposed to face this problem, either based on measuring (destructively) and partially recreating the signal [5,6], sharing entanglement over large distances [7–10] or pairing coding [11]. The above schemes are referred to as quantum repeaters.

In this paper we address devices which, besides extracting information, preserves, at least in part, the entire quantum state of the signal, i.e., the statistics of *all* possible observables. Our device thus conveys characteristics of both quantum nondemolition (QND) measurements of a given observable, and classical repeaters, whose goal is to preserve the global information carried by a signal. Since the main feature of our scheme is the tunability of the information–disturbance tradeoff [12], without any specific focus on the measurement, we do not refer to them as QND schemes, whose goal is limited to preserve the statistics of a specific observable.

The tradeoff between information gain and quantum state disturbance can be quantified in different ways [13]; here we

use fidelities, which may be defined as follows. Suppose one wants to transmit the symbol a, chosen from the alphabet $\mathbb{A}$ according to the probability density $p(a)$. To this aim a quantum system is prepared in the pure state $|\psi_a\rangle$, chosen from a given set, and then transmitted along a given channel. In order to share the information among several users one needs a device which couples the signal to one or more probe systems in order to produce two outputs. One of the two outputs is sent to a user, who measures a predetermined observable to infer the transmitted state, whereas the (conditional) state of the second output is left to the subsequent user and thus should contain an approximate copy of the input signal. If the outcome b is observed after the device, then the estimated signal state is given by $|\phi_b\rangle$ (a *natural* inference rule being $b \rightarrow |\phi_b\rangle$ with $|\phi_b\rangle$ given by the set of eigenstates of the measured observable), whereas the conditional state $|\varphi_b\rangle$ is left for the subsequent user. The amount of disturbance is quantified by evaluating the overlap of the conditional state $|\varphi_b\rangle$ to the initial one $|\psi_a\rangle$, whereas the amount of information extracted by the measurement corresponds to the overlap of the inferred state $|\phi_b\rangle$ to the initial one. The corresponding fidelities, for a given input signal $|\psi_a\rangle$, are given by

$$F_a = \int_{\mathbb{B}} db\, q(b) |\langle \varphi_b | \psi_a \rangle|^2, \tag{1}$$

$$G_a = \int_{\mathbb{B}} db\, q(b) |\langle \phi_b | \psi_a \rangle|^2, \tag{2}$$

where we have already performed the average over the distribution $q(b)$ of the outcomes. The alphabet $\mathbb{B}$ of the output symbols (i.e., the spectrum of the measured observable) is not necessarily equal to the input one, though this choice is an optimized one [14]. The relevant quantities to assess the performances of the scheme are then given by the average fidelities

*Electronic address: matteo.paris@fisica.unimi.it

$$F = \int_A \int_B da\,db\,p(a)q(b)|\langle\varphi_b|\psi_a\rangle|^2, \qquad (3)$$

$$G = \int_A \int_B da\,db\,p(a)q(b)|\langle\phi_b|\psi_a\rangle|^2, \qquad (4)$$

which are obtained by averaging F_a and G_a over the possible input states, i.e., over the alphabet $\mathbb{A}$ of transmittable symbols. F will be referred to as the *transmission fidelity* and G as the *estimation fidelity*. Of course we have $0 \le G \le 1$ and $0 \le F \le 1$ with $F=1$ corresponding to zero disturbance and $G=1$ to complete information.

Our device is local and its action is independent of the presence of losses along the transmission line. The presence of losses before the device degrades the signals and, as a matter of fact, is equivalent to consider a set of mixed states at the input. The performance of such a device can be obtained from the analysis of the pure state case by averaging the fidelity over the input probability. The result is an overall degradation of performances. Since our focus is on exploring the ultimate bounds imposed by quantum mechanics, we are not going to take into account the mixing at the input. In the following, we consider a scheme suitable to transmit a continuous alphabet $\mathbb{A}$, whose symbols are encoded in a set of Gaussian pure states of a continuous variable (CV) infinite dimensional system.

Let us first consider the extreme case: if nothing is done, the signal is preserved $\forall a$ and thus $F=1$. However, at the same time, our estimation has to be random, and thus $G \to 0$ since we are dealing with an infinite-dimensional system. This corresponds to a *blind* regeneration scheme [15], which reprepares any quantum state received at the input, without gaining any information on it. The opposite case is when the maximum information is gained on the signal, i.e., when the optimal estimation strategy for the parameter of interest is adopted [16,17]. In this case $G \neq 0$, but then the signal after this operation cannot provide any more information on the initial state. Our aim is to study intermediate cases, i.e., quantum measurements providing only partial information while partially preserving the quantum state of the signal for subsequent users. These kinds of schemes, which correspond to feasible quantum measurements, may be also viewed as universal quantum nondemolition measurements [18] (i.e., not built for a specific observable), which have been widely investigated for CV systems, and recently received attention also for qubits [19–21].

For discrete variable, the tradeoff between information gain and state disturbance has been explicitly evaluated [4], as well as the bound that fidelities should satisfy according to quantum mechanics. In turn, optimal schemes for finite-dimensional systems (qudits), i.e., devices whose fidelity balance saturates the bound have been suggested [12,24] (in Ref. [12] those schemes have been referred to as *optimal quantum repeaters*).

As a matter of fact the fidelity bound for finite-dimensional systems cannot be straightforwardly extended to infinite dimension, and no analog bound has been derived for CV systems, except for the case of coherent states in phase-

insensitive devices [22] and non-Gaussian protocol [23]. Therefore, in order to gain insight on the fidelity balance for CV systems and to clarify the role of energy allocation, in this paper we suggest a class of *minimal* schemes which involve a single additional probe, and evaluate their performances as a function of the channel (signal and probe) energy, which, in turn, depends on the *width* of the signal and the probe wave packets as well as the *size* of the alphabet. Indeed energy constraints are the main focus in infinite-dimensional systems, and may serve to define optimality [25].

The paper is structured as follows: In Sec. II we describe our schemes and evaluate the probability of the outcomes as well as the corresponding conditional states, whereas in Sec. III we evaluate fidelities and analyze the information–disturbance tradeoff in terms of the signal and the probe energy for different configurations. In Sec. IV we discuss the optical implementation of our schemes, whereas Sec. V closes the paper with some concluding remarks.

II. CONTINUOUS VARIABLE INDIRECT MEASUREMENTS

In this section we suggest a measurement scheme suitable to infer the information carried by a class of Gaussian CV states without destroying the signals themselves. The setup is the generalization to infinite dimension of the optimal schemes suggested in Ref. [12] for qudits. The setup is minimal because it involves a single additional probe system.

A. Input signals

We consider the transmission of a real alphabet $\mathbb{A} \equiv \mathbb{R}$ with symbols a encoded in the set of Gaussian signals

$$|\psi_{a\tau}\rangle_s = \int dx\,g_{a,\tau}(x)|x\rangle_s, \qquad (5)$$

where $|x\rangle$ denotes the standard CV basis, say position eigenstates, with $\langle x'|x\rangle = \delta(x-x')$ and

$$|g_{a,\tau}(x)|^2 = \frac{1}{\sqrt{2\pi}\tau}\exp\left[-\frac{(x-a)^2}{2\tau^2}\right].$$

The label s indicates signal quantities throughout the paper. We assume, without loss of generality, $g_{a,\tau}(x)$ as real, i.e., that the signal states $|\psi_{a\tau}\rangle_s$ are Gaussian wave-packets centered in a, with zero "momentum" and a fixed width τ. We also assume that the *a priori* probability $p(a)$ of the symbol a, i.e., the probability to have a signal centered in a, is given by a Gaussian

$$p(a) = \frac{1}{\sqrt{2\pi}\Delta}\exp\left(-\frac{a^2}{2\Delta^2}\right)$$

of zero mean and width Δ. The width Δ will be referred to as the *size* of the transmitted alphabet. Notice that the class $\{|\psi_{a\tau}\rangle_s\}$ is made by nonorthogonal states, and we have.

$$\left|{}_s\langle\psi_{b\tau'}|\psi_{a\tau}\rangle_s\right|^2 = \frac{2\tau\tau'}{\tau^2+\tau'^2}\exp\left\{-\frac{(a-b)^2}{2(\tau^2+\tau'^2)}\right\},$$
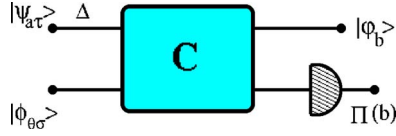
and, in particular,

FIG. 1. (Color online) Schematic diagram of an indirect measurement scheme for continuous variable systems. The symbols from the input alphabet $\mathbb{A}$ are encoded in a set of Gaussian signals $|\psi_{a\tau}\rangle_s$ with real amplitude a and fixed width τ. The a priori probability of the transmitted symbols is a Gaussian with zero mean and width Δ. The signal is coupled, by a C_{sum} gate, to a probe excited in the known state $|\phi_{\theta\sigma}\rangle_p$. After the interaction the probe is measured in order to infer the transmitted state, while the signal is left for the subsequent user. The measurement is described by the operator-valued measure $\Pi(b)$, which is optimized in order to maximize the estimation fidelity. The output signals $|\varphi_b\rangle_s$ are the conditional states of the signal after having observed the outcome b.

$$|_s\langle\psi_{b\tau}|\psi_{a\tau}\rangle_s|^2 = \exp\left\{-\frac{(a-b)^2}{4\tau^2}\right\}.$$

Upon defining the standard dual basis, say momentum eigenstates, as

$$|p\rangle = \frac{1}{\sqrt{2\pi}}\int dx e^{ipx}|x\rangle, \qquad (6)$$

one has that the position- and momentumlike observables are given by

$$X = \int dx x|x\rangle\langle x|, \quad P = \int dp p|p\rangle\langle p|,$$

whereas the energy operator reads as follows: $N=\frac{1}{2}(X^2+P^2)$. The average energy $N_s(a)=_s\langle\psi_{a\tau}|N|\psi_{a\tau}\rangle_s$ of the signal is thus given by

$$N_s(a) = \frac{1}{2}\left(a^2 + \tau^2 + \frac{1}{4\tau^2}\right).$$

Finally, the mean energy sent into the channel per use (from now on the signal energy) reads as follows:

$$N_s = \int da p(a) N_s(a) = \frac{1}{2}\left(\Delta^2 + \tau^2 + \frac{1}{4\tau^2}\right).$$

For each signal $|\psi_{a\tau}\rangle_s$ we have $\Delta X^2=\tau^2$ and $\Delta P^2=(4\tau^2)^{-1}$ that is, the signals $|\psi_{a\tau}\rangle_s$ are minimum uncertainty states. For $\tau^2=1/2$ one has equal variances, whereas $\tau^2 \neq 1/2$ corresponds to "squeezing" of the signals. The signal energy is minimum for $\tau^2=1/2$; in this case we have $N_s=\frac{1}{2}(1+\Delta^2)$.

Notice that transmitted symbols may be viewed as shift parameters $|\psi_{a\tau}\rangle_s=\exp(-iPa)|\psi_{0\tau}\rangle_s$ imposed to the "undisplaced" basic state $|\psi_{0\tau}\rangle_s$. This feature will be used in optimizing the measurement at the output.

B. Preparation of the probe state

The setup of the measurement scheme is shown in Fig. 1. The signal is coupled with a probe system excited in the (known) state

$$|\phi_{\theta\sigma}\rangle_p = \cos\theta\int dx g_{0,\sigma}(x)|x\rangle_p + \gamma\sin\theta\int dp g_{0,\sigma}(p)|p\rangle_p$$

$$= \int dx[\cos\theta g_{0,\sigma}(x) + \gamma\sin\theta g_{0,(2\sigma)^{-1}}(x)]|x\rangle_p, \qquad (7)$$

where $\theta\in[0,\pi/2]$, and

$$\gamma = \frac{\sqrt{1+\beta^2\tan^2\theta}-1}{\beta\tan\theta}, \quad \beta^2 = \sigma^2 + \frac{1}{4\sigma^2} \qquad (8)$$

is a normalization factor.

The state $|\phi_{\theta\sigma}\rangle_p$, in close analogy with the finite-dimensional case [12], is built as a tunable superposition of the almost localized state (up to the width σ) $|\phi_{0\sigma}\rangle_p$ and the almost delocalized state $|\phi_{0(2\sigma)^{-1}}\rangle_p$. The probe state depends on two parameters: θ and the width σ. This apparent redundancy can be eliminated upon imposing a constraint on the probe energy $N_p(\sigma,\theta)=_p\langle\phi_{\theta\sigma}|N|\phi_{\theta\sigma}\rangle_p$, whose expression reads as follows:

$$N_p(\beta,\theta) = \frac{1}{2}\left[\beta^2(\cos^2\theta + \gamma^2\sin^2\theta) + \frac{\gamma}{\beta^3}\sin 2\theta\right]$$

$$= \frac{1}{2}\left[\beta^2 + \frac{2\cos^2\theta(\beta^4-1)}{\beta^4}(1 - \sqrt{1+\beta^2\tan^2\theta})\right]. \qquad (9)$$

At a fixed value of θ the probe energy is minimum for $\sigma^2=1/2$ ($\beta=1$), corresponding to $N_p(1,\theta)=\frac{1}{2}$, whereas at a fixed value of σ the probe energy is minimum for

$$\tan^2\frac{\theta}{2} = 1 + 2\frac{\beta - \sqrt{2\beta(1+\beta)}}{2+\beta} \qquad (10)$$

corresponding to $N_p(\beta)=\frac{1+\beta(\beta-1)(\beta^2+1)}{2\beta^2}$.

The two-parameter nature of the probe signal will be used to analyze the information–disturbance tradeoff in different configurations, which include regimes at fixed energy as well as regime with increasing energy.

C. Interaction

The signal and the probe are then coupled by a $C_{\mathrm{sum}}=\exp\{-iX_s\otimes P_p\}$ gate (denoted by C in Fig. 1), which acts on the standard basis of the signal-probe system as follows:

$$C_{\mathrm{sum}}|x\rangle_s|y\rangle_p = |x\rangle_s|x+y\rangle_p,$$

i.e., represents the generalization to the continuous variable of the C_{not} gate. [26]. The global (entangled) signal-probe state $|\psi_{\mathrm{out}}\rangle\rangle_{sp}$ after the interaction is given by

$$|\psi_{\mathrm{out}}\rangle_{sp} = C|\psi_{a\tau}\rangle_s \otimes |\phi_{\theta\sigma}\rangle_p$$

$$= \cos\theta\int\int dx dy g_{\sigma,0}(x)g_{a,\tau}(y)|y\rangle_s \otimes |x+y\rangle_p$$

$$+ \frac{\gamma\sin\theta}{\sqrt{2\pi}}\int\int\int dp dx' dy g_{0,\sigma}(p)g_{a,\tau}(y)e^{ipx'}|y\rangle_s$$

$$\otimes |x'+y\rangle_p$$

$$= \int \int dx dy g_{a,\tau}(y)[\cos \theta g_{0,\sigma}(x)$$

$$+ \gamma \sin \theta g_{0,(2\sigma)^{-1}}(x)]|y\rangle_s \otimes |x + y\rangle_p. \quad (11)$$

D. Measurement

After the interaction the probe is measured in order to infer the transmitted state, while the signal is left for the subsequent user. The measurement is described by the operator-valued measure $P(b) = I \otimes \Pi(b)$, where $\Pi(b)$ is an operator-valued measure acting on the sole probe Hilbert space. Since the transmitted symbols are Gaussian distributed shift parameters we expect the optimal measurement to be of the form [16]

$$\Pi(b) = \frac{1}{\kappa}|b/\kappa\rangle_{pp}\langle b/\kappa|$$

with $|b\rangle_p$ being the standard basis states (position eigenstates) and κ a real constant, hereafter referred to as the measurement gain, chosen to optimize the desired figure of merit (here the estimation fidelity). In order to estimate the transmitted state from the outcomes of the measurement we assume the natural inference rule

$$b \rightarrow |\psi_{b\tau}\rangle_s,$$

where $|\psi_{b\tau}\rangle_s$ is of the form (5), i.e., a signal Gaussian wave packet centered in b and width τ. The probability density $q(b)$ of obtaining the outcome b, and the expression of the corresponding conditional state ϱ_b for the signal are thus given by

$$q(b) = \text{Tr}_{sp}[|\psi_{\text{out}}\rangle\rangle_{sp\ sp}\langle\langle\psi_{\text{out}}|\mathbb{I} \otimes \Pi(b)] = {}_s\langle\widetilde{\varphi}_b|\widetilde{\varphi}_b\rangle_s, \quad (12)$$

$$\varrho_b = \frac{1}{q(b)} \text{Tr}_p[|\psi_{\text{out}}\rangle\rangle_{sp\ sp}\langle\langle\psi_{\text{out}}|\mathbb{I} \otimes \Pi(b)$$

$$= \frac{1}{q(b)}|\widetilde{\varphi}_b\rangle_{ss}\langle\widetilde{\varphi}_b| = |\varphi_b\rangle_{ss}\langle\varphi_b|. \quad (13)$$

The last equalities in both Eqs. (12) and (13), which express the purity of the conditional state, follow from the fact that the initial states of both the signal and the probe are pure, and that the measure $\Pi(b)$ is pure too. Mixed measurements may be considered as well, though unavoidably leading to additional *extrinsic* noise [16,17]. The unnormalized signal states $|\widetilde{\varphi}_b\rangle_s$ are given by

$$|\widetilde{\varphi}_b\rangle_s = \frac{1}{\sqrt{\kappa}^p}\langle b|\psi_{\text{out}}\rangle\rangle_{sp}$$

$$= \frac{\cos \theta}{\sqrt{\kappa}} \int \int dx dy g_{\sigma,0}(x)g_{a,\tau}(y) \delta(b/\kappa - x - y)|y\rangle_s$$

$$+ \frac{\gamma \sin \theta}{\sqrt{2\pi\kappa}} \int \int \int dp dx' dy g_{0,\sigma}(p)g_{\sigma,a}(y)e^{ipx'} \delta(b/\kappa$$

$$- x' - y)|y\rangle_s$$

$$= \int \frac{dy}{\sqrt{\kappa}} g_{a,\tau}(y)[\cos \theta g_{b/\kappa,\sigma}(y) + \gamma \sin \theta g_{b/\kappa,(2\sigma)^{-1}}(y)]|y\rangle_s$$

$$(14)$$

thus leading to

$$q(b) = \frac{1}{\kappa} \int dy |g_{a,\tau}(y)|^2 [\cos \theta g_{b/\kappa,\sigma}(y) + \gamma \sin \theta g_{b/\kappa,(2\sigma)^{-1}}(y)]^2.$$

$$(15)$$

In Eqs. (12)–(14), for the sake of a simpler notation, we omitted the explicit dependence of the conditional states on the signal and probe widths, τ and σ.

III. INFORMATION–DISTURBANCE TRADEOFF

We are now in the position of evaluating the fidelities. As a concern of the transmission fidelity, according to Eq. (1) we have

$$F_a = \int db q(b)|_s\langle\varphi_b|\psi_{a\tau}\rangle_s|^2 = \int db |_s\langle\widetilde{\varphi}_b|\psi_{a\tau}\rangle_s|^2.$$

After lengthy but straightforward calculations one arrives at

$$F_a = \frac{\sqrt{2}\sigma \cos^2 \theta}{\sqrt{2\sigma^2 + \tau^2}}$$

$$+ \frac{4\sigma \cos \theta(-2\sigma \cos \theta + \sqrt{1 + 4\sigma^4 - (1 - 2\sigma^2)^2 \cos^2 \theta})}{\sqrt{(1 + 4\sigma^4)(1 + 4\sigma^4 + 4\sigma^2\tau^2)}}$$

$$+ \frac{(-2\sigma \cos \theta + \sqrt{1 + 4\sigma^4 - (1 - 2\sigma^2)^2 \cos^2 \theta})^2}{(1 + 4\sigma^4)\sqrt{1 + 2\sigma^2\tau^2}}. \quad (16)$$

Notice that F_a does not depend on the amplitude a, nor on the measurement gain κ. Therefore the average fidelity F

$$F = \int da p(a)F_a = F_a,$$

is equal to the signal fidelity and also does not depend on the alphabet size Δ.

Using Eqs. (2) and (15) one evaluates the estimation fidelity G_a as follows:

$$G_a = \int db q(b)|_s\langle\psi_{b\tau}|\psi_{a\tau}\rangle_s|^2. \quad (17)$$

The signal fidelity G_a depends on the amplitude a of the signal, by averaging over the *a priori* signal probability $p(a)$ we arrive at the estimation fidelity G,

$$G = \int da\, p(a) G_a = \frac{\sqrt{2}\tau\cos^2\theta}{\sqrt{\Delta^2(\kappa-1)^2 + 2\tau^2 + \kappa^2(\sigma^2 + \tau^2)}} - \frac{\sqrt{2}\tau\cos^2\theta(8\sigma^2 - 4\sigma\sqrt{4\sigma^2 + (1+4\sigma^4)\tan^2\theta})}{\sqrt{(1+4\sigma^4)(\Delta^2(\kappa-1)^2(1+4\sigma^4) + 2(1+4\sigma^4)\tau^2 + \kappa^2(2\sigma^2 + \tau^2 + 4\sigma^4\tau^2))}}$$
$$+ \frac{\sqrt{2}\tau\cos^2\theta[16\sigma^3 + 2(\sigma + 4\sigma^5)\tan^2\theta - 8\sigma^2\sqrt{4\sigma^2 + (1+4\sigma^4)\tan^2\theta}]}{(1+4\sigma^4)\sqrt{4\sigma^2(\Delta^2 + 2\tau^2) + \kappa^2(1 + 4\Delta^2\sigma^2 + 4\sigma^2\tau^2) - 8\kappa\Delta^2\sigma^2}}, \tag{18}$$

which, besides the signal and probe widths, depends on the alphabet size Δ and the measurement gain κ.

By inspecting Eqs. (16) and (18) the superposition nature of the probe state $|\phi_{\theta\sigma}\rangle_p$ can be clearly seen; at fixed values of the parameters κ and Δ the fidelities oscillate as a function of the tuning parameter θ (see Fig. 2). As it is apparent from the plots for $\sigma^2 < 1/2$ the transmission (estimation) fidelity F (G) is maximized (minimized) at $\theta = \pi/2$ and is minimized (maximized) at $\theta = 0$, whereas for $\sigma^2 > 1/2$ the situation is the opposite. By varying the values of κ and Δ the shape of the curves slightly change, while the overall behavior is the same.

In order to derive a proper information–disturbance tradeoff we first have to optimize (maximize) the estimation fidelity with respect to the measurement gain κ. The general solution of the optimization equation is rather involved and does not offer a clear picture. Therefore, in order to gain insight on the general behavior, we now proceed to analyze the optimization and the corresponding tradeoffs for relevant configurations.

A. Probe in the high-energy limit

In order to compare the optimal scheme for qudit to the present CV scheme we start by considering the probe in the state

$$|\psi_{\theta 0}\rangle = \cos\theta |0\rangle_p + \frac{\sin\theta}{\sqrt{2\pi}} \int dx\, |x\rangle_p, \tag{19}$$

which is the plain analog of the probe used in the optimal scheme for the qudit [12]. We obtain this configuration by taking the limit $\sigma \to 0$ in (7). Of course this is an ideal case, since it corresponds to a probe state with divergent energy. As it concerns the optimization of the measurement we obtain

$$\kappa_{\rm opt} = \frac{\Delta^2}{\Delta^2 + \tau^2} \tag{20}$$

which corresponds to fidelities

$$F = \sin^2\theta, \tag{21}$$

$$G = \cos^2\theta \sqrt{\frac{1 + \dfrac{\Delta^2}{\tau^2}}{1 + \dfrac{3}{2}\dfrac{\Delta^2}{\tau^2}}} \tag{22}$$

and to the parametric function $F = F_A(G, y)$,

$$F_A(G, y) = 1 - G\sqrt{\frac{1 + \dfrac{3}{2}y}{1 + y}}, \quad y = \frac{\Delta^2}{\tau^2}, \tag{23}$$

which depends on the ratio y between the alphabet size and the signal width. We have a linear dependence between the two fidelities and for each curve one can explore the tradeoff by varying the parameter θ; one moves along the curve from right to left by increasing θ. Different curves for different values of the ratio y are depicted in Fig. 3. We see that the high-fidelity region (both F and G close to unity) is excluded and that the tradeoff is better for small values of the ratio y, i.e., for "small alphabets." For increasing y, i.e., for increasing the size of the alphabet, the slope of the curve $F_A(G, y)$ decreases. The function $F_A(G, y)$ intercepts the G axis at $G = \sqrt{(1+y)/(1+\frac{3}{2}y)}$.

B. Probe in the undisplaced state

Here we analyze the case of undisplaced probe state $|\phi_{0\sigma}\rangle_p$ which, in the limit $\sigma \to 0$ approaches the localized state $|0\rangle_p$. We can obtain this configuration by setting $\theta = 0$ in Eq. (7). Maximizing the estimation fidelity with respect to the measurement gain we arrive at

$$\kappa_{\rm opt} = \frac{\Delta^2}{\Delta^2 + \tau^2 + \sigma^2}$$

and, correspondingly, to the fidelities

$$F = \sqrt{\frac{2z}{1 + 2z}}, \quad z = \frac{\sigma^2}{\tau^2}, \tag{24}$$

$$G = \sqrt{\frac{1 + z + y}{1 + z + \dfrac{y}{2}(3 + z)}}, \tag{25}$$

which, besides the ratio y, also depend on the ratio z between the probe and the signal widths.

Upon inverting Eq. (25) we arrive at the parametric function $F = F_B(G, y)$, which depends only on the ratio y,

$$F_B(G, y) = \sqrt{\frac{G^2(4 + 6y) - 4(1 + y)}{G^2(2 + 5y) - 4\left(\dfrac{1}{2} + y\right)}}. \tag{26}$$

In Fig. 4 we show the tradeoff for different values of y.

As it is apparent from the plot, this configuration allows us to achieve the high-fidelity region. The tradeoff is worse
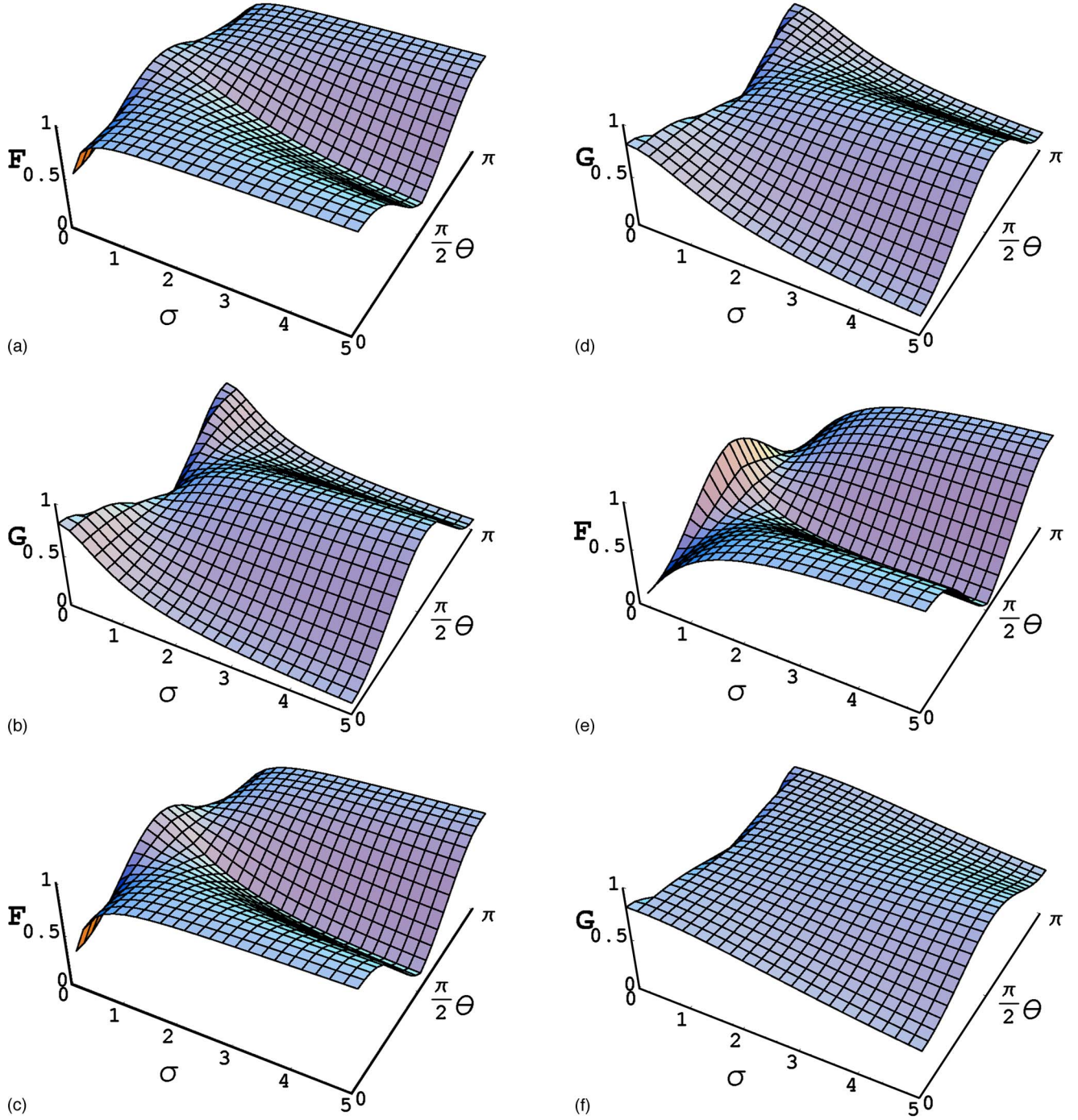
FIG. 2. (Color online) Left: Transmission fidelity $F(\sigma,\theta)$ for $\kappa=1$ and for different values of τ, from top to bottom $\tau=0.4, 1/\sqrt{2}, 2$. Right: Estimation fidelity $G(\sigma,\theta)$ for $\kappa=1$, $\Delta=1/\sqrt{2}$ and for different values of τ; from top to bottom $\tau=0.4, 1\sqrt{2}, 2$.

for larger values of the ratio between the alphabet size and the signal width. Therefore, in order to get superior performances, it is preferable to have a small alphabet rather than a class of narrow signals. For fixed width of the signals this is intuitively expected; the larger the alphabet the worse the tradeoff. On the other hand, for a fixed alphabet size, this means that the larger the signals the better the tradeoff. One moves along each curve by tuning the probe width σ; from right to left by increasing σ.

C. Probe in the minimum energy state

As we have already seen, at fixed θ we have minimum energy for $\sigma^2=1/2$. In this case we also lose the dependency on θ and the probe state is given by

$$|\phi_{\theta 2^{-1/2}}\rangle_p = \int dx\, g_{0,2^{-1/2}}(x)|x\rangle_p.$$

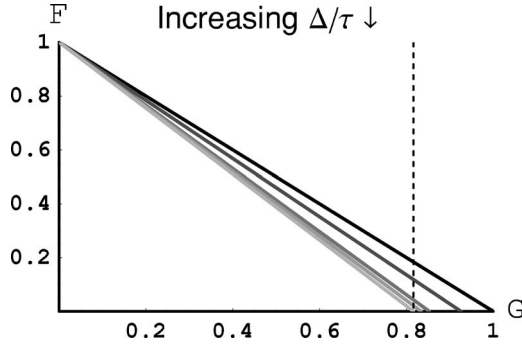The optimal κ is given by

FIG. 3. Information–disturbance tradeoff $F_A(G, y)$ in the high energy limit for the probe, for different values of the width ratio $y = \Delta^2/\tau^2$. From darker to lighter gray we plot the tradeoff for $y = 0.5, 3, 7, 10\,000$. The tradeoff gets worse for increasing values of y. For $y \gg 1$ the function $F_A(G, y)$ intercepts the axis $F = 0$ for $G = \sqrt{2/3}$. One moves along the curve, from right to left, by increasing θ.

$$\kappa_{\text{opt}} = \frac{2\Delta^2}{1 + 2\Delta^2 + 2\tau^2}, \tag{27}$$

which corresponds to fidelities
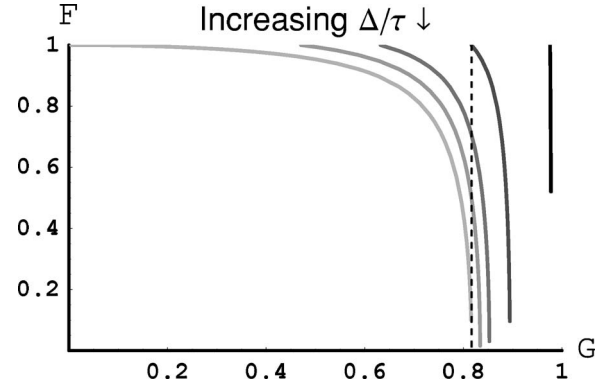
$$F = \sqrt{\frac{1}{1 + \tau^2}}, \tag{28}$$

FIG. 4. Information–disturbance tradeoff $F_B(G, y)$ for the probe in the undisplaced state $|\psi_{0\sigma}\rangle_p$ and for different values of the ratio $y = \Delta^2/\tau^2$. From darker to lighter gray: the tradeoff for $y = 0.1, 1, 3, 7, 10\,000$. The tradeoff gets worse for increasing values of y. For $y \gg 1$ the function $F_B(G, y)$ intercepts the G axis at $G = \sqrt{2/3}$. One moves along the curves from right to left by increasing σ.

$$G = \tau \sqrt{\frac{2(1 + 2\Delta^2 + 2\tau^2)}{4\tau^4 + \Delta^2 + 2\tau^2(1 + 3\Delta^2)}}, \tag{29}$$

and to the parametric function

$$F_C(G, \Delta) = \sqrt{\frac{3 - 2\Delta^2 + 3G^2(\Delta^2 - 1) - \sqrt{(1 + 2\Delta^2)^2 - 2G^2(1 + 3\Delta^2 + 6\Delta^4) + G^4(1 + 2\Delta^2 + 9\Delta^4)}}{2 - 4\Delta^2 + G^2(5\Delta^2 - 2)}}. \tag{30}$$

The tradeoff $F_C(G, \Delta)$, which depends only on the alphabet size Δ, is shown for different values of Δ in Fig. 5.

Also this configuration permits to access the high-fidelity region. The curves corresponding to smaller values of Δ are
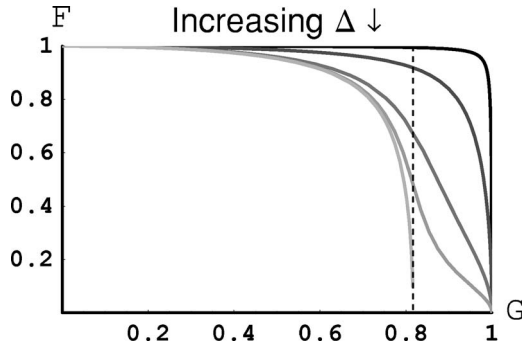

FIG. 5. Information–disturbance tradeoff $F_C(G, \Delta)$ for the probe with minimum energy and for different values of the alphabet width Δ. From darker to lighter gray: the tradeoff for $\Delta = 0.1, 0.2, 2, 5, \infty$. The tradeoff gets worse for increasing values of Δ. For $\Delta \to \infty$ the function $F_C(G, \Delta)$ intercepts the G axis at $G = \sqrt{2/3}$. One moves along the curves from left to right by increasing τ.

the upper ones, i.e., the tradeoff is worse for larger alphabets. One moves along the curves by tuning the signal width τ, from left to right by increasing τ. For narrower signal we have less disturbances, though we get less information too. In the limit for $\Delta \to 0$ we have $F_C(G, 0) = 1$, in particular, up to the second order in Δ (see Fig. 5, upper curve) we have

$$F_C(G, \Delta) = 1 + \frac{G^2}{4(G^2 - 1)}\Delta^2 + O(\Delta^4). \tag{31}$$

For uniform alphabets, i.e., in the limit $\Delta \to \infty$, Eq. (30) rewrites as

$$F = \sqrt{\frac{4 - 6G^2}{4 - 5G^2}}. \tag{32}$$

We may assume Eq. (32) as the CV bound for signals chosen from a flat distribution in the Hilbert space. This should be compared with the rigorous bound derived in Ref. [4] for random qudits, i.e., for signals uniformly distributed in a d-dimensional Hilbert space
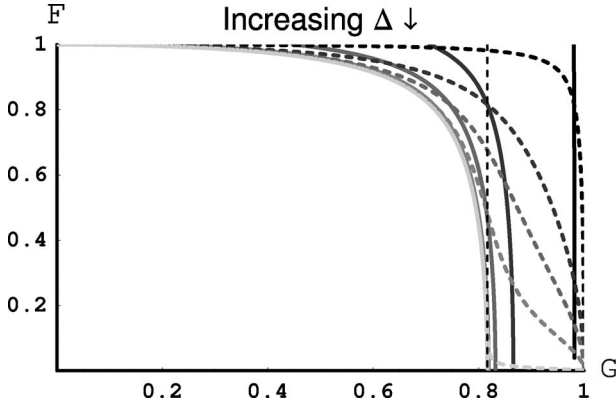
FIG. 6. Information–disturbance tradeoffs $F_B(G, 2\Delta^2)$ and $F_C(G, \Delta)$ (dashed lines) for different values of Δ. From darker to lighter gray: the tradeoffs for $\Delta = 0.2, 1, 2, 5, 100$. For $\Delta \gtrsim 3$ the two configurations lead to similar results. For $\Delta < 3$ configuration B favors the information fidelity whereas configuration C privileges the estimation fidelity.

$$F = \frac{1}{d+1} + \left(\sqrt{G - \frac{1}{d+1}} + \sqrt{(d-1)\left(\frac{2}{d+1} - G\right)} \right)^2.$$
(33)

A continuous-variable system thus appears to offer the possibility of a superior tradeoff at the price of increasing the energy impinged into the device. Notice, however, that increasing the probe energy does not necessarily lead to better tradeoff, e.g., compare Eq. (23) to Eqs. (26) and (30). On the other hand, the tradeoff strongly depends on the ratio between the alphabet size and the signal width, which in turn determine the allocation of the signal energy.

D. Comparison between different probe configurations

Here we compare the tradeoffs achievable by setting the probe in the undisplaced state $|\phi_{0\sigma}\rangle_p$ (configuration B) and in the minimum energy state $|\phi_{\theta 2^{-1/2}}\rangle_p$ (configuration C), respectively. Since (26) depends on the ratio Δ/τ and (30) depends only on Δ we compare the two configurations by fixing the signal width. The value $\tau^2 = 1/2$ has been chosen in order to have signals with minimum energy. The trade-off $F_B(G, y)$ rewrites as

$$F = F_B(G, 2\Delta^2) = \sqrt{\frac{2(G^2(3\Delta^2 - 1) + 1 - 2\Delta^2)}{G^2(5\Delta^2 + 1) - 4\Delta^2 - 1}}.$$

In Fig. 6 the tradeoffs are compared for different values of Δ.

For alphabet sizes larger than a threshold $\Delta \gtrsim \Delta_{th}$ the curves are very similar, approximately leading to the same tradeoff. On the other hand, for $\Delta < \Delta_{th}$ configuration B favors the information fidelity whereas configuration C privileges the estimation fidelity. For $\tau^2 = 1/2$ we have roughly $\Delta_{th} \simeq 3$.

IV. OPTICAL IMPLEMENTATION

In this section we briefly mention how the building blocks of our scheme can be implemented in a quantum optical scenario. The main goal is to show that the present scheme may be implemented with currently technology, rather than describing a specific measurement scheme.

The measurement in the standard basis corresponds to homodyne detection, whereas the signals $|\psi_{a\tau}\rangle$ are Gaussian wave packets with amplitude a and width τ. They correspond to squeezed-coherent states of the form $D(a/\sqrt{2})S(r)|0\rangle$ where $|0\rangle$ is the em vacuum, $D(\alpha) = \exp(\alpha a^\dagger - \bar{\alpha}a)$ is the displacement operator and $S(r) = \exp\left[\frac{1}{2}(\zeta a^{\dagger 2} - \bar{\zeta}a^2)\right]$ is the squeezing operator. In order to obtain the signals $|\psi_{a\tau}\rangle$, the relation $\sinh^2 r = \frac{1}{2}(\tau^2 + \frac{1}{4\tau^2})$ must hold. As it concerns the interaction, the C-sum gate $C_{sum} = \exp\{-iX_s \otimes P_p\}$ expressed in terms of the mode operators reads as follows: $C_{sum} = \exp\{\frac{1}{2}(a^\dagger b^\dagger + ab^\dagger - ab - a^\dagger b)\}$ and may be implemented by parametric interactions in a second order $\chi^{(2)}$ nonlinear crystals. Alternatively, conditional schemes involving both linear and nonlinear interactions have been also proposed [27,28]. As a matter of fact, C_{sum} interaction between light pulses has been investigated in several previous experiments [29]. In addition, it has been experimentally observed between the polarization of light pulses and collective spin of huge atomic samples [30].

V. CONCLUSIONS

We have suggested a class of indirect measurement schemes to estimate the state of a continuous variable Gaussian system without destroying the state itself. The schemes involve a single additional probe and allow for the nondemolitive transmission of a continuous real alphabet over a quantum channel. The tradeoff between information gain and state disturbance has been quantified by fidelities and optimized with respect to the measurement performed after the signal-probe interaction. Different configurations have been analyzed in terms of the energy carried by the signal and the probe. A bound for a class of randomly distributed CV signals has been derived, which may be compared with the analogous (general) bound derived for qudits [4]. We found that a continuous-variable system generally offers the possibility of a better tradeoff at the price of increasing the overall energy introduced into the device. Notice, however, that increasing the probe energy does not necessarily lead to a better tradeoff, the most relevant parameter being the ratio between the alphabet size and the signal width, which in turn determines the allocation of the signal energy.

[1] H. F. Hofmann, Phys. Rev. A **62**, 022103 (2000).

[2] W. K. Wootters and W. K. Zurek, Nature (London) **299**, 802 (1982); V. Buzek and M. Hillery, Phys. Rev. A **54**, 1844 (1996); N. Gisin and S. Massar, Phys. Rev. Lett. **79**, 2153 (1997); R. F. Werner, Phys. Rev. A **58**, 1827 (1998).

[3] M. Murao *et al.*, Phys. Rev. A **59**, 156 (1999); P. vanLoock and S. Braunstein, Phys. Rev. Lett. **87**, 247901 (2001); A. Ferraro *et al.*, J. Opt. Soc. Am. B **21**, 1241 (2004).

[4] K. Banaszek, Phys. Rev. Lett. **86**, 1366 (2001).

[5] J. F. Roch, J. P. Poizat, and P. Grangier, Phys. Rev. Lett. **71**, 2006 (1993).

[6] Y. Yamamoto, Science **263**, 1394 (1994).

[7] H. J. Briegel, W. Dur, J. I. Cirac, and P. Zoller, Phys. Rev. Lett. **81**, 5932 (1998).

[8] L. Childress, J. M. Taylor, A. S. Srensen, and M. D. Lukin, quant-ph/0410123.

[9] L. Childress, J. M. Taylor, A. S. Srensen, and M. D. Lukin, Phys. Rev. Lett. **95**, 030503 (2005).

[10] P. Kok, C. P. Williams, and J. P. Dowling, Phys. Rev. A **68**, 022301 (2003).

[11] B.-S. Shi, Y.-K. Jiang, and G.-C. Guo, Physica A **284**, 107 (2000).

[12] M. G. Genoni and M. G. A. Paris, Phys. Rev. A **71**, 052307 (2005).

[13] H. F. Hofmann, Phys. Rev. A **67**, 022106 (2003).

[14] C. M. Caves and P. D. Drummond, Rev. Mod. Phys. **66**, 481 (1994).

[15] M. G. A. Paris, Fortschr. Phys. **51**, 202 (2003).

[16] C. W. Helstrom, *Quantum Detection and Estimation Theory* (Academic, New York, 1976).

[17] A. S. Holevo, *Statistical Structure of Quantum Theory* (Springer-Verlag, Berlin, 2001).

[18] V. B. Braginsky, Yu. I. Vorontsov, and K. S. Thorne, Science **209**, 547 (1980); M. F. Bocko and R. Onofrio, Rev. Mod. Phys. **68**, 755 (1996); See also the special issue on QND, J. Mlynek *et al.*, Appl. Phys. B: Lasers Opt. **B64**, 123 (1997).

[19] T. C. Ralph, S. D. Bartlett, J. L. O'Brien, G. J. Pryde, and H. M. Wiseman, Phys. Rev. A **73**, 012113 (2006).

[20] P. Kok, H. Lee, and J. P. Dowling, Phys. Rev. A **66**, 063814 (2002).

[21] G. J. Pryde, J. L. O'Brien, A. G. White, S. D. Bartlett, and T. C. Ralph, Phys. Rev. Lett. **92**, 190402 (2004).

[22] U. L. Andersen, M. Sabuncu, R. Filip, and G. Leuchs, Phys. Rev. Lett. **96**, 020409 (2006).

[23] L. Mišta, quant-ph/0510191.

[24] L. Mišta and R. Filip, Phys. Rev. A **72**, 034307 (2005).

[25] A. Ferraro, S. Olivares, and M. G. A. Paris, *Gaussian States in Quantum Information* (Bibliopolis, Napoli, 2005).

[26] S. D. Bartlett, B. C. Sanders, S. L. Braunstein, and K. Nemoto, Phys. Rev. Lett. **88**, 097904 (2002).

[27] G. M. D'Ariano and M. F. Sacchi, Phys. Lett. A **231**, 325 (1997).

[28] Matteo G. A. Paris, Phys. Rev. A **65**, 012110 (2002).

[29] S. F. Pereira *et al.*, Phys. Rev. Lett. **72**, 214 (1994); K. Bencheikh *et al.*, *ibid.* **75**, 3422 (1995); K. Bencheikh *et al.*, *ibid.* **78**, 34 (1997); R. Bruckmeier *et al.*, *ibid.* **78**, 1243 (1997); R. Filip, quant-ph/0404010.

[30] L.-M. Duan *et al.*, Phys. Rev. Lett. **85**, 5643 (2000); A. Kuzmich and E. S. Polzik, *ibid.* **85**, 5639 (2000); B. Julsgaard *et al.*, Nature (London) **413**, 400 (2001); C. Schori *et al.*, Phys. Rev. Lett. **89**, 057903 (2002).